

Modular pulse programme generation for NOAH supersequences

Jonathan R. J. Yong,¹ Ēriks Kupče,² Tim D. W. Claridge^{1,*}

¹ Chemistry Research Laboratory, Department of Chemistry, University of Oxford, Mansfield Road, Oxford, OX1 3TA, U.K.

² Bruker UK Ltd., Banner Lane, Coventry, CV4 9GH, U.K.

* tim.claridge@chem.ox.ac.uk

Abstract

(132 words)

NOAH (NMR by Ordered Acquisition using ^1H -detection) supersequences allow multiple 2D NMR datasets to be acquired in greatly reduced experiment durations through the elision of recovery delays. In NOAH experiments, up to five “modules” can be combined, which means that there is a very large number of plausible supersequences (over 4000). This renders the traditional method of pulse programme construction by hand wholly inadequate. We introduce here a tool named GENESIS (GENEration of Supersequences In Silico), available via <https://nmr-genesis.co.uk>, which programmatically generates arbitrary NOAH supersequences compatible with Bruker spectrometers. This not only allows users to obtain customised supersequences for specific applications, but also enables us to rapidly and effortlessly disseminate new NOAH modules (e.g. PSYCHE, 2D J) as well as improvements to old modules (e.g. ^{13}C - ^1H HMBC, ^{15}N - ^1H HMQC).

1 Introduction

The acceleration of NMR data acquisition has in recent years proven a fruitful area for NMR pulse sequence and method development, particularly for n -dimensional ($n\text{D}$) NMR where raw data is acquired as a series of increments. Developments in this area include (but are not limited to) ultrafast NMR,^{1–3} non-uniform sampling (NUS),^{4–6} multiple-FID experiments,^{7–10} and the shortening or elision of recovery delays.^{11–14} In this paper, we focus on NOAH (NMR by Ordered Acquisition using ^1H -detection) experiments,^{15–22} which fall under the last two categories. NOAH experiments consist of a series of up to five 2D experiments (“modules”), combined into one single “supersequence” which uses only one recovery delay for all modules. This provides substantial (up to 4×) time savings compared to conventional acquisition, in which one recovery delay is used for each module (Figure 1).

Virtually all common 2D experiments have been implemented in NOAH supersequences to date, including HMBC, HSQC, HSQC-TOCSY, HMQC, COSY, TOCSY, NOESY, and ROESY. Each module is given a unique abbreviation, usually one letter long (e.g. ‘B’ for HMBC, ‘S’ for HSQC,

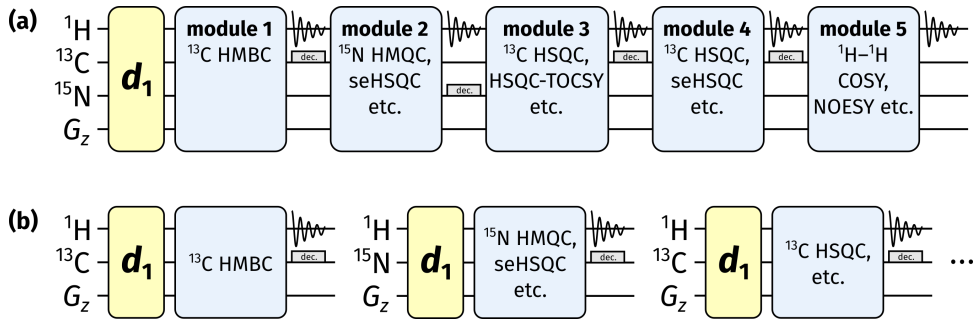


Figure 1: (a) Diagrammatic representation of a NOAH supersequence, where only one recovery delay (d_1) is used for the entire experiment. (b) Conventional 2D NMR data acquisition, where one recovery delay is used per dataset.

'M' for HMQC, 'C' for COSY) and occasionally sub/superscripted (e.g. 'S^T' for HSQC-TOCSY or 'S⁺' for seHSQC). The combinatorial nature of NOAH experiments means that there are a very large number of conceivable supersequences ranging from NOAH-2 to NOAH-5 (where the suffix indicates the number of modules). In principle, this figure is on the order of N^5 , where N is the number of available modules: as of the time of writing, N is 27, which in total yields more than 10 million NOAH supersequences.

For optimal data quality in terms of both sensitivity and artefact minimisation, there are certain conditions on NOAH supersequences. Specifically, NOAH modules placed earlier in a supersequence should ideally utilise only the specific magnetisation they require. As a concrete example, in the NOAH-2 SC supersequence (HSQC and COSY), the ^1H - ^{13}C HSQC module is designed to excite only the ^1H nuclei directly attached to the 1.1%-natural abundance ^{13}C and leave all other proton magnetisation (the "bulk magnetisation") along the equilibrium +z axis.¹³ A ^1H - ^1H COSY module (or TOCSY, or NOESY, etc.) can then draw on this bulk magnetisation, with almost no loss in sensitivity and without having to wait for the ^{13}C -bound protons to relax. Conversely, if the COSY module were placed first, the ^{13}C -bound proton magnetisation would not survive for use in the HSQC: thus, the HSQC module in a NOAH-2 CS would display severe sensitivity losses, as compared to in a NOAH-2 SC. More subtle factors are also abound, such as in the SBC sequence,¹⁵ where COSY intensities are modulated by T_2 relaxation and J_{HH} evolution. The alternative BSC arrangement,¹⁶ especially with isotropic "ASAP" mixing applied before the COSY, circumvents this issue and has become the preferred implementation for HMBC/HSQC combinations.¹⁷

Considerations such as these restrict the set of "effective" NOAH supersequences. Even so, the original NOAH paper alone suggests a figure of 285,¹⁵ and the number of available modules has only grown since then. By our calculations, as of the time of writing, there are 4242 "optimal" NOAH supersequences (Section S1). Constructing every one of these supersequences "by hand" is clearly unreasonable. Consequently, it has not been possible to disseminate an exhaustive series of pulse programmes: we have so far had to limit ourselves to a handful of "typical" supersequences, which may or may not be applicable to users' needs. To solve this problem, we sought to *programmatically* generate NOAH pulse programmes, in a way which

GENESIS: a NOAH pulse programme generator

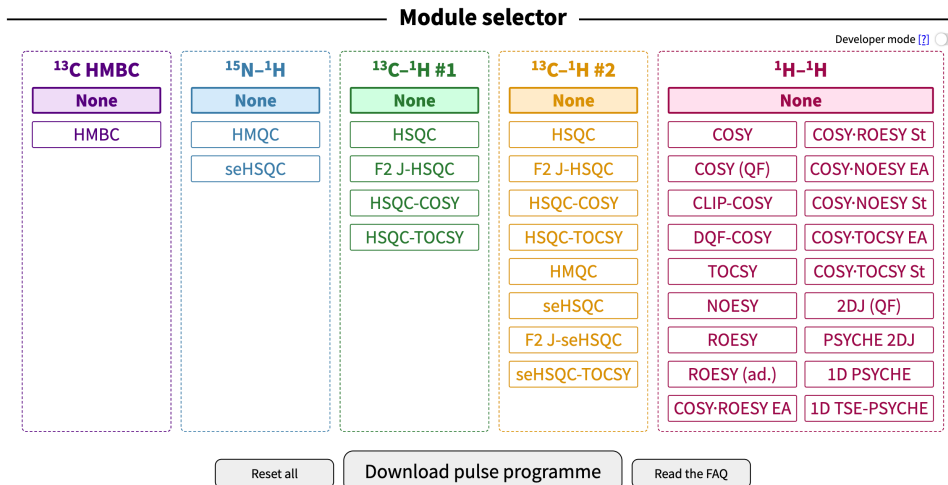


Figure 2: A screenshot of the GENESIS web interface. Visible here are the module choices, the “developer mode” toggle, and buttons for downloading the pulse programme.

makes new combinations as easy as possible to set up and minimises the chances of human error. We term this approach GENESIS (GENEration of Supersequences In Silico). The implementation of this is a single web page (Figure 2), accessible via <https://nmr-genesis.co.uk>, which can construct virtually any supersequence one might want. The regular user interface is designed to only produce “optimal” supersequences: thus, for example, it is not possible to create the CS or SBC supersequences discussed earlier. This is most useful for ordinary users who wish to follow established best practices. For more advanced usage, enabling “developer mode” will remove these limitations, allowing any arbitrary combination of modules to be created.

2 Implementation details

We begin with a brief discussion of how the GENESIS approach works. The pulse programme generation code itself is written in TypeScript (version 4.2.3, Microsoft), which is compiled to JavaScript (formally ECMAScript 2015, or “ES6”) and then executed directly in a client’s browser; there is no server-side code. The web browser shows a list of modules for users to choose from, using accessible and familiar names such as HMBC, HSQC, and so on (Figure 2). Internally, these are mapped to a series of NOAHModule objects, each of which contain module-specific information, such as its abbreviation, the requisite parameter definitions, the pulse programme for the module itself, and the appropriate AU programme to be used for processing.

Using this information, GENESIS then constructs the pulse programme in several steps (Figure 3):

```

; noah2-SpCc
; 13C sensitivity-enhanced HSQC
; [use -DEDIT for multiplicity editing]
; 1H CLIP-COSY (States)

① define delay DC_SEHSQCa
② "d4      = 0.25s/cnst2" ; 13C INEPT
   "DC_SEHSQCa = d4-p14/2" ; zz-filter
   "l0      = td1/2"        ; TD1/NBL

③ 1 ze
4 50u UNBLKGRAD
; Module 1 - 13C seHSQC
(p1 ph0):f1
DC_SEHSQCa
goscnp ph30 cpd2:f2
50u do:f2
2m st
; Module 2 - CLIP-COSY
(p1 ph6):f1
go=2 ph26
④ 1m igrad EA
if "l1 % 2 == 0" {
  1m id0
  1m id10
}
  lo to 4 times l0
exit

⑤ ph0=0
ph1=1

⑥ ;gpnam0: SMSQ10.100
;gpz0: 29% (for purging)
⑦ ;sp3:wvm:wu180C13: cawurst-20(60 kHz, 0.5 ms; L2H)
⑧ ;d0: 13C t1
;d4: 1/4J(CH)
⑨ ;auprog: noah_hsqc:noah_clipcosy States
;module identifiers: C_SEHSQC H_CLIP_COSY
;pulse programme created by genesis-v2.0.12, https://nmr-genesis.co.uk
;Sun Sep 12 2021 21:03:34 GMT+0100 (British Summer Time)

```

Figure 3: Abridged pulse programme for a NOAH-2 S⁺C^c supersequence (¹³C seHSQC + CLIP-COSY). Specific sections of interest are numbered on the left. (1) Module-specific delays are given unique identifiers to prevent clashes and to improve readability. (2) TopSpin parameters (delays such as d4) are standardised between modules. (3) The pulse programme instructions themselves begin here. (4) *t*₁ incrementation and echo-antiecho gradient inversion is carried out with the appropriate frequency (once per loop or once per two loops). (5) Pulse and receiver phase cycles are standardised between modules. (6) Comments for gradient pulses are compatible with the TopSpin gppp script. (7) Instructions for generating shaped pulses using TopSpin's WaveMaker software. (8) Comments describing each parameter appear in the parameter setup screen. (9) Instructions for processing AU programmes (Section 3.4) are encoded here, along with information about the specific modules used and a timestamp which ensures reproducibility.

- Header comments including information about the pulse programme and constituent modules;
- Parameter definitions from each module are then collated, taking particular care to avoid duplicate definitions for parameters used in multiple modules;
- The main section, which contains the actual instructions for the pulse sequence, is then put together. This is done mostly by concatenating individual modules together, although there are also context-sensitive blocks placed *between* modules such as purge pulses, gradients, or ASAP mixing¹⁷ in BSX-type supersequences (X being any homonuclear module);
- Appropriate looping and incrementation of parameters such as phase cycles, t_1 delays, and gradient amplitudes for echo–antiecho selection is added at the end of the main section;
- Additional comments containing descriptive text for parameters (displayed in TopSpin’s ase parameter setup screen), as well as gradient and shaped pulse information (which allow direct setup using the gppp and wvm commands), are added at this stage. These are collated by scanning the main section for TopSpin parameters (e.g. delays, pulses, gradients) and obtaining their descriptions from a lookup table;
- Finally, to ensure full reproducibility in the pulse programme generation, we also specify the exact modules used in the pulse programme, the GENESIS version number, and a timestamp.

The website further contains a series of frequently asked questions and instructions on how to set NOAH experiments up. It also offers download links for the AU scripts used for processing, as well as the new Python script used for toggling non-uniform sampling on/off (noah_nus2.py, discussed in Section 3.5).

2.1 Standardisation of parameter meanings

An immediate problem of directly concatenating pulse programme texts from different modules is that a given parameter in one module may take on a different value in another module. As a necessary step to prevent such clashes, we have fully standardised all parameters used in the GENESIS pulse programmes. These include pulse widths (p), delays (d), constants (cnst), z-gradient amplitudes (gpz), and phase cycles (ph). Thus, d2 is always $1/(2 \cdot {}^1J_{CH})$, and d4 is always $1/(4 \cdot {}^1J_{CH})$. Where possible, we have chosen meanings that are similar to those in the standard library of Bruker pulse programmes. However, there are invariably some small deviations: for example, the Δ' delay in the ${}^{13}\text{C}$ sensitivity-enhanced HSQC (which can range from $1/(8 \cdot {}^1J_{CH})$ to $1/(4 \cdot {}^1J_{CH})$)²³ is d24 in the standard library, but we have chosen d6 because d24 is reserved for $1/(4 \cdot {}^1J_{NH})$.

In place of module-specific delays which are often called DELTA1, ... in standard library se-

quences, we have chosen to define new identifiers with more human-readable names inside the pulse programme itself. Thus, the delays in a HSQC sequence might be called DC_HSQC1, ..., where the first C indicates the indirect-dimension nucleus (^{13}C).

While this standardisation was primarily implemented in order to facilitate pulse programme construction, this also makes it far easier for users to set up a series of different supersequences, as virtually every parameter value can simply be reused between experiments. In principle, it is possible to set up a single “prototype” parameter set which already has every parameter set up; to run a different NOAH experiment, one need only change PULPROG, TD1, NBL, and any sample-specific parameters.

2.2 Choice of module ‘versions’

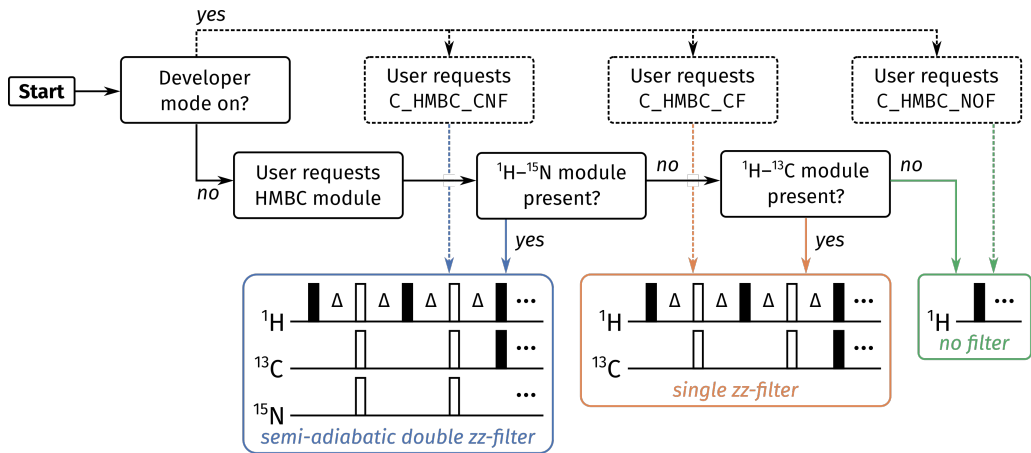


Figure 4: Flowchart illustrating how GENESIS decides the form of the zz-filter to be used in a HMBC module. Dotted lines represent the branch where developer mode is enabled, i.e. the user has full control over which form is used: these are labelled by alphabetical codes starting with C_HMBC (the website contains a full description of these codes). Solid lines represent the branch where developer mode is not enabled: in this case, GENESIS chooses the appropriate module based on what other modules are present in the supersequence.

Another potential issue is that different versions of a pulse sequence often exist. A simple example is the zz-HMBC,^{16,18} where the zz-filter element is used to retain ^{13}C -bound and optionally ^{15}N -bound ^1H magnetisation, depending on what modules follow. Since the user only specifies that they want a HMBC module and not the exact details of the zz-filter, the GENESIS code must in effect make this choice for the user (Figure 4). The sensitivity-enhanced HSQC (seHSQC, abbreviated ‘S⁺/Sp) presents a similar case. If the seHSQC module is followed by one or more homonuclear modules such as a COSY or NOESY, then the ZIP-seHSQC^{21,22} should be used, as this preserves the requisite magnetisation for the later modules. However, if the seHSQC module is used last in the sequence, then the original Cavanagh–Rance–Kay seHSQC^{24,25} should be used in order to maximise sensitivity.

3 Other NOAH improvements

A substantial benefit of the GENESIS approach is that it provides a single source for all NOAH pulse sequences and processing scripts, which are always in sync with one another. This allows us to rapidly disseminate new NOAH developments to users, independently from TopSpin's own release cycle, and without needing a separate publication for each. The initial GENESIS release already contains a number of such improvements, some of which we detail below.

3.1 Suppression of one-bond artefacts in HMBC

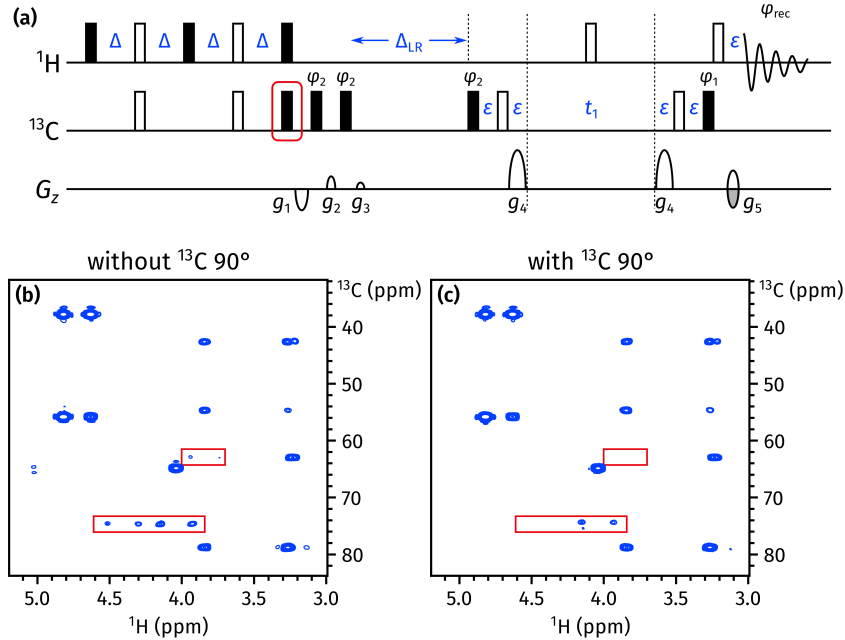


Figure 5: (a) The NOAH *zz*-HMBC pulse sequence, with the newly added ¹³C 90° pulse highlighted in red. The delays are $\Delta = 1/(4 \cdot ^1J_{\text{CH}})$ and $\Delta_{\text{LR}} = 1/(2 \cdot ^nJ_{\text{CH}})$; ε is the minimum time required for a gradient plus the subsequent recovery delay. Phase cycling is performed as follows: $\phi_1 = x, -x$; $\phi_2 = x, x, -x, -x$; $\phi_{\text{rec}} = x, -x, -x, x$. All gradients have duration 1 ms; amplitudes as a fraction of the maximum gradient strength (55.7 G/cm) are as follows: $g_1 = -15\%$; $g_2 = 10\%$; $g_3 = 5\%$; $g_4 = 80\%$; $g_5 = \pm 40.2\%$. (b) HMBC spectrum obtained using the original *zz*-HMBC module, i.e. without the added 90° pulse. ¹J_{CH} artefacts are highlighted in red boxes. (c) HMBC spectrum obtained with the added 90° pulse. Spectra were obtained on a 700 MHz Bruker AV III equipped with a TCI H/C/N cryoprobe; the sample used was 40 mM andrographolide in DMSO-*d*₆.

The *zz*-HMBC module is ordinarily placed first in a supersequence, where the *zz*-filter element serves to preserve magnetisation of protons directly coupled to ¹³C and/or ¹⁵N.^{16,18} Specifically, the *zz*-filter acts as a 90° excitation pulse on uncoupled protons, while leaving coupled protons along +*z*. This is largely accomplished in practice, as evidenced by the fact that the intensities in subsequent HSQC-type modules are barely perturbed. However, not all of the coupled magnetisation is perfectly retained: in particular, the *zz*-filter also generates a degree of *antiphase* magnetisation of the form $2\text{H}_x\text{C}_z$. This antiphase magnetisation is later refocused during the low-pass J-filter (LPJF) to give in-phase magnetisation, eventually ending up as one-

bond correlation artefacts in the HMBC spectrum (Figure 5b).

A simple solution to this is to add a ^{13}C 90° pulse at the end of the zz -filter (Figure 5a): this converts any antiphase magnetisation to double- or zero-quantum magnetisation, which is later destroyed by the LPJF. This idea has previously been used by Luy and coworkers in CLIP-HSQC experiments to remove antiphase contributions prior to FID detection.²⁶ In the event, this small modification proved to have a large impact, almost completely suppressing the $^1\text{J}_{\text{CH}}$ artefacts (Figure 5c). Further comparisons of artefact intensity are provided in Section S2.

3.2 ^{15}N HMQC gradient scheme

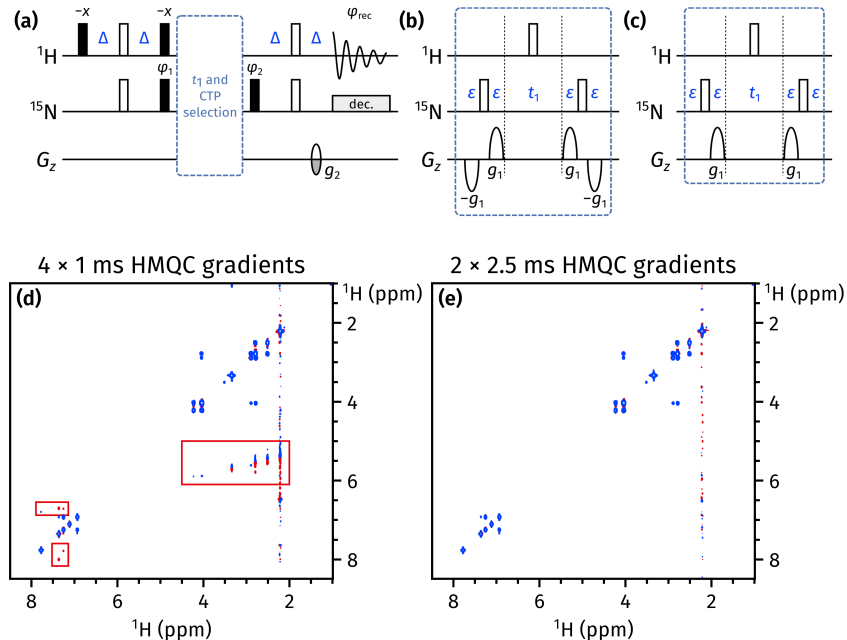


Figure 6: (a) A general outline of the NOAH ^{15}N HMQC module. g_2 has a duration which matches that of g_1 (explained below), and an amplitude of $\pm n \cdot 8.1\%$, where n is the number of CTP gradients bracketing the t_1 period. g_1 has an amplitude of 80% in all cases. All other symbols have the same meaning as in Figure 5. (b) The previously published coherence selection scheme for the HMQC module, with four gradients each of duration 1 ms. (c) The new coherence selection scheme for the HMQC module, with two gradients each of duration 2.5 ms. (d)–(e) CLIP-COSY spectra obtained from a NOAH-3 MS⁺C supersequence (^{15}N HMQC + ^{13}C seHSQC + CLIP-COSY), acquired with the gradient schemes shown in (b) and (c) respectively. The wing artefacts in the former spectrum are highlighted in red boxes. Spectra were obtained on a 700 MHz Bruker AV III equipped with a TCI H/C/N cryoprobe; the sample used was 50 mM zolmitriptan in DMSO- d_6 .

We have recently described the occurrence of “wing artefacts” in homonuclear modules, which arise from bulk magnetisation which evolves during either half of t_1 in a preceding heteronuclear module.²² These artefacts can be removed in an elegant manner by ensuring that each half of t_1 in a HMQC/HSQC/seHSQC module contains coherence transfer pathway (CTP) gradients of equal sign and magnitude, which makes sure that any bulk magnetisation undergoing net evolution during t_1 is dephased.

At the same time, it is also important that the final gradient in the heteronuclear module have as large an amplitude as possible, since this gradient is responsible for dephasing bulk magnetisation that is not returned to $+z$ just prior to the detection period. In order to accomplish this, the previous ^{15}N HMQC module used bipolar opposing gradients in either half of t_1 , a scheme which allows the final refocusing CTP gradient g_2 to have an amplitude of $4g_1(\gamma_{\text{N}}/\gamma_{\text{H}})$ (Figure 6b). Although this leads to excellent artefact suppression in the ^{15}N HMQC itself, wing artefacts are apparent in downstream modules (Figure 6d), because the opposing gradients cancel each other out and do not enforce any CTP selection on the bulk magnetisation.

The solution to this is to only use two gradients during t_1 (one in either half), and to *lengthen* their duration such that the final gradient g_2 provides sufficient dephasing in the HMQC itself (Figure 6c). This strategy was previously described for the ^{15}N seHSQC;²² here we have also applied it to the HMQC with success (Figure 6e). This change causes no significant difference in the sensitivity of the HMQC module itself (Figure S3).

3.3 PSYCHE and 2DJ modules

In previous work,²² we described how $^1\text{H}-^{15}\text{N}$ modules could be implemented with optional “ k -scaling”.²⁷ This entails a reduction in the number of t_1 increments (by a factor of k), in return for a corresponding increase in the number of transients per increment, with no overall change in the experimental time. Particularly for the HMQC experiment, this allowed modest gains in sensitivity as J_{HH} splittings were no longer resolved in the indirect dimension.

A simple extension of this protocol to *homonuclear* $^1\text{H}-^1\text{H}$ modules enables experiments such as 2D J-resolved or pseudo-2D pure shift spectroscopy to be incorporated into NOAH supersequences. In both cases, the number of t_1 increments needed (16–32) is far smaller than the typical number required for a 2D experiment (128–256). In particular, at present, we have implemented a family of PSYCHE experiments, namely the original pseudo-2D PSYCHE, the triple spin echo (TSE)-PSYCHE experiment which provides improved robustness towards strong coupling, and the PSYCHE 2DJ experiment which yields pure absorption-mode lineshapes.^{28–30}

In PSYCHE spectra, the flip angle of the chirp or saltire pulses used in the J-refocusing element provides the experimentalist with a choice: a larger flip angle provides greater sensitivity, but at the cost of increased artefacts.³⁰ One advantage of acquiring PSYCHE spectra in NOAH-type supersequences is that, due to the increased number of transients, sensitivity is often not at a premium. Thus, the user can choose a smaller flip angle (ca. 10°) in order to maximise spectral purity instead, while not losing any actual spectrometer time. An example of a NOAH-3 supersequence with the TSE-PSYCHE module is shown in Figure 7.

3.4 splitx_au processing

NOAH data processing is done using the `splitx_au` AU programme; this is responsible for creating NBL separate datasets containing the data for each module, and processing each dataset

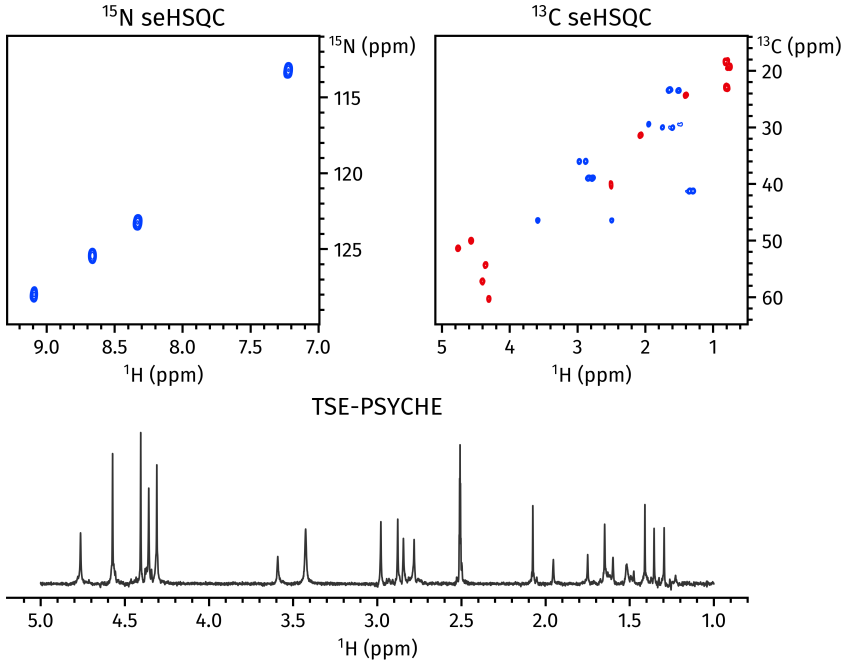


Figure 7: Spectra obtained from a NOAH-3 $S_N^+S^+P^T$ supersequence. (a) ¹⁵N sensitivity-enhanced HSQC²² (256 t_1 increments, 2 scans per increment). (b) ¹³C sensitivity-enhanced HSQC^{21,22} (256 t_1 increments, 2 scans per increment). (c) 1D TSE-PSYCHE pure shift spectrum²⁸ (saltire flip angle of 10°, 32 chunks, 16 scans per chunk). Spectra were obtained on a 700 MHz Bruker AV III equipped with a TCI H/C/N cryoprobe; the sample used was 40 mM gramicidin in DMSO- d_6 .

using module-specific AU programmes (e.g. noah_hsqc for ¹³C HSQC data). Previously, the module-specific AU programmes had to be specified as the USERP1, USERP2, ... series of processing parameters. Since the GENESIS approach allows module-specific information such as these to be embedded within the pulse programme itself, this means that (with a small modification to the splitx_au AU programme) we can parse the pulse programme to obtain the requisite list of AU programmes. The user therefore does not have to specify it explicitly, which makes setting up multiple different supersequences a much smoother process. It is still possible to specify the USERPx parameters, and these will override the AU programmes parsed from the pulse programme, but in practice there is no real reason to do so.

3.5 Non-uniform sampling implementation

With the GENESIS pulse programmes we also introduce a new and more user-friendly implementation of non-uniform sampling (NUS). NOAH experiments do not work “out of the box” with TopSpin’s conventional NUS setup routine: some special adjustments have to be made by manually generating the list of increments to be sampled and adjusting the t_1 delays accordingly. Previously, this was accomplished using a Python script which created a new pulse programme for each supersequence, e.g. noah3_BSC.nus.¹⁷ We have modified this approach such that the *same* pulse programme can be used for both uniform and non-uniform sampling, where NUS is controlled by an acquisition flag -DNUS. Although a (different) Python script is

still required for initialisation, this means that it is no longer necessary to keep two separate instances of the same pulse sequence in TopSpin, and reduces the difficulty of turning NUS on and off.

4 Conclusion

Here, we have demonstrated how the programmatic generation of NOAH pulse programmes can be used to create any supersequence that users are interested in (of which there are thousands). Furthermore, we have described several improvements to NOAH modules along with the associated processing routines; these are already available via the GENESIS website (<https://nmr-genesis.co.uk>).

In its current form, GENESIS is not capable of creating arbitrary pulse sequences. However, this remains a viable target for the future: instead of combining NOAH modules to form a supersequence, one may instead consider combining pulse sequence elements to form a single sequence. [...]

References

- (1) Frydman, L.; Scherf, T.; Lupulescu, A. *Proc. Natl. Acad. Sci. U. S. A.* **2002**, *99*, 15858–15862, DOI: [10.1073/pnas.252644399](https://doi.org/10.1073/pnas.252644399).
- (2) Frydman, L.; Lupulescu, A.; Scherf, T. *J. Am. Chem. Soc.* **2003**, *125*, 9204–9217, DOI: [10.1021/ja030055b](https://doi.org/10.1021/ja030055b).
- (3) Tal, A.; Frydman, L. *Prog. Nucl. Magn. Reson. Spectrosc.* **2010**, *57*, 241–292, DOI: [10.1016/j.pnmrs.2010.04.001](https://doi.org/10.1016/j.pnmrs.2010.04.001).
- (4) Mobli, M.; Hoch, J. C. *Prog. Nucl. Magn. Reson. Spectrosc.* **2014**, *83*, 21–41, DOI: [10.1016/j.pnmrs.2014.09.002](https://doi.org/10.1016/j.pnmrs.2014.09.002).
- (5) Kazimierczuk, K.; Orekhov, V. *Magn. Reson. Chem.* **2015**, *53*, 921–926, DOI: [10.1002/mrc.4284](https://doi.org/10.1002/mrc.4284).
- (6) Gołowicz, D.; Kasprzak, P.; Orekhov, V.; Kazimierczuk, K. *Prog. Nucl. Magn. Reson. Spectrosc.* **2020**, *116*, 40–55, DOI: [10.1016/j.pnmrs.2019.09.003](https://doi.org/10.1016/j.pnmrs.2019.09.003).
- (7) Nolis, P.; Pérez-Trujillo, M.; Parella, T. *Angew. Chem. Int. Ed.* **2007**, *46*, 7495–7497, DOI: [10.1002/anie.200702258](https://doi.org/10.1002/anie.200702258).
- (8) Kupče, Ě.; Freeman, R. *J. Am. Chem. Soc.* **2008**, *130*, 10788–10792, DOI: [10.1021/ja8036492](https://doi.org/10.1021/ja8036492).
- (9) Nagy, T. M.; Gyöngyösi, T.; Kövér, K. E.; Sørensen, O. W. *Chem. Commun.* **2019**, *55*, 12208–12211, DOI: [10.1039/c9cc06253j](https://doi.org/10.1039/c9cc06253j).
- (10) Nagy, T. M.; Kövér, K. E.; Sørensen, O. W. *J. Magn. Reson.* **2020**, *316*, 106767, DOI: [10.1016/j.jmr.2020.106767](https://doi.org/10.1016/j.jmr.2020.106767).
- (11) Schanda, P.; Van Melckebeke, H.; Brutscher, B. *J. Am. Chem. Soc.* **2006**, *128*, 9042–9043, DOI: [10.1021/ja062025p](https://doi.org/10.1021/ja062025p).

- (12) Kupče, Ē.; Freeman, R. *Magn. Reson. Chem.* **2007**, *45*, 2–4, DOI: [10.1002/mrc.1931](https://doi.org/10.1002/mrc.1931).
- (13) Schulze-Sünninghausen, D.; Becker, J.; Luy, B. *J. Am. Chem. Soc.* **2014**, *136*, 1242–1245, DOI: [10.1021/ja411588d](https://doi.org/10.1021/ja411588d).
- (14) Nagy, T. M.; Kövér, K. E.; Sørensen, O. W. *Angew. Chem. Int. Ed.* **2021**, *60*, 13587–13590, DOI: [10.1002/anie.202102487](https://doi.org/10.1002/anie.202102487).
- (15) Kupče, Ē.; Claridge, T. D. W. *Angew. Chem. Int. Ed.* **2017**, *56*, 11779–11783, DOI: [10.1002/anie.201705506](https://doi.org/10.1002/anie.201705506).
- (16) Kupče, Ē.; Claridge, T. D. W. *Chem. Commun.* **2018**, *54*, 7139–7142, DOI: [10.1039/c8cc03296c](https://doi.org/10.1039/c8cc03296c).
- (17) Claridge, T. D. W.; Mayzel, M.; Kupče, Ē. *Magn. Reson. Chem.* **2019**, *57*, 946–952, DOI: [10.1002/mrc.4887](https://doi.org/10.1002/mrc.4887).
- (18) Kupče, Ē.; Claridge, T. D. W. *J. Magn. Reson.* **2019**, *307*, 106568, DOI: [10.1016/j.jmr.2019.106568](https://doi.org/10.1016/j.jmr.2019.106568).
- (19) Kupče, Ē.; Mote, K. R.; Webb, A.; Madhu, P. K.; Claridge, T. D. W. *Prog. Nucl. Magn. Reson. Spectrosc.* **2021**, *124-125*, 1–56, DOI: [10.1016/j.pnmrs.2021.03.001](https://doi.org/10.1016/j.pnmrs.2021.03.001).
- (20) Kupče, Ē.; Frydman, L.; Webb, A. G.; Yong, J. R. J.; Claridge, T. D. W. *Nat. Rev. Methods Primers* **2021**, *1*, No. 27, DOI: [10.1038/s43586-021-00024-3](https://doi.org/10.1038/s43586-021-00024-3).
- (21) Hansen, A. L.; Kupče, Ē.; Li, D.-W.; Bruschweiler-Li, L.; Wang, C.; Brüschweiler, R. *Anal. Chem.* **2021**, *93*, 6112–6119, DOI: [10.1021/acs.analchem.0c05205](https://doi.org/10.1021/acs.analchem.0c05205).
- (22) Yong, J. R. J.; Hansen, A. L.; Kupče, Ē.; Claridge, T. D. W. *J. Magn. Reson.* **2021**, *329*, 107027, DOI: [10.1016/j.jmr.2021.107027](https://doi.org/10.1016/j.jmr.2021.107027).
- (23) Schleucher, J.; Schwendinger, M.; Sattler, M.; Schmidt, P.; Schedletzky, O.; Glaser, S. J.; Sørensen, O. W.; Griesinger, C. *J. Biomol. NMR* **1994**, *4*, 301–306, DOI: [10.1007/BF00175254](https://doi.org/10.1007/BF00175254).
- (24) Palmer III, A. G.; Cavanagh, J.; Wright, P. E.; Rance, M. *J. Magn. Reson.* **1991**, *93*, 151–170, DOI: [10.1016/0022-2364\(91\)90036-s](https://doi.org/10.1016/0022-2364(91)90036-s).
- (25) Kay E., L.; Keifer, P.; Saarinen, T. *J. Am. Chem. Soc.* **1992**, *114*, 10663–10665, DOI: [10.1021/ja00052a088](https://doi.org/10.1021/ja00052a088).
- (26) Enthart, A.; Freudenberger, J. C.; Furrer, J.; Kessler, H.; Luy, B. *J. Magn. Reson.* **2008**, *192*, 314–322, DOI: [10.1016/j.jmr.2008.03.009](https://doi.org/10.1016/j.jmr.2008.03.009).
- (27) Pérez-Trujillo, M.; Nolis, P.; Bermel, W.; Parella, T. *Magn. Reson. Chem.* **2007**, *45*, 325–329, DOI: [10.1002/mrc.1973](https://doi.org/10.1002/mrc.1973).
- (28) Foroozandeh, M.; Adams, R. W.; Kiraly, P.; Nilsson, M.; Morris, G. A. *Chem. Commun.* **2015**, *51*, 15410–15413, DOI: [10.1039/c5cc06293d](https://doi.org/10.1039/c5cc06293d).
- (29) Foroozandeh, M.; Adams, R. W.; Meharry, N. J.; Jeannerat, D.; Nilsson, M.; Morris, G. A. *Angew. Chem. Int. Ed.* **2014**, *53*, 6990–6992, DOI: [10.1002/anie.201404111](https://doi.org/10.1002/anie.201404111).
- (30) Foroozandeh, M.; Morris, G. A.; Nilsson, M. *Chem. Eur. J.* **2018**, *24*, 13988–14000, DOI: [10.1002/chem.201800524](https://doi.org/10.1002/chem.201800524).

Supporting Information

for

Modular pulse programme generation for NOAH supersequences

Jonathan R. J. Yong,¹ Ēriks Kupče,² Tim D. W. Claridge^{1,*}

¹ *Chemistry Research Laboratory, Department of Chemistry, University of Oxford,
Mansfield Road, Oxford, OX1 3TA, U.K.*

² *Bruker UK Ltd., Banner Lane, Coventry, CV4 9GH, U.K.*

* tim.claridge@chem.ox.ac.uk

S1 Number of combinations

In this section we count the total number of “plausible” NOAH combinations, available from the non-developer mode version of the GENESIS website, using the inclusion–exclusion principle. As of version 2.0.12 of the website, there are five categories of modules:

- HMBC (2 choices, including “none”)
- $^{15}\text{N}-^1\text{H}$ (3 choices, including “none”)
- $^{13}\text{C}-^1\text{H} \#1$ (5 choices, including “none”)
- $^{13}\text{C}-^1\text{H} \#2$ (9 choices, including “none”)
- $^1\text{H}-^1\text{H}$ (19 choices, including “none”)

To a first approximation, there are therefore $2 \cdot 3 \cdot 5 \cdot 9 \cdot 19 = 5130$ combinations. Since we included the “none” options in this product, this figure includes “lesser” supersequences such as NOAH-4 and lower. However, this does contain some invalid combinations, namely:

1. All five “none” modules selected (1).
2. “NOAH-1” combinations with only one module: $1 + 2 + 4 + 8 + 18 = 33$. These are technically valid experiments (and the pulse programmes generated by the website *will* function correctly), but they are no different from standard 2D experiments so the NOAH description does not truly apply to these.
3. “NOAH-6” combinations where there is one experiment in each of the first four categories, and a “double” experiment (e.g. COSY + NOESY) in the last category. There are 6 such modules, for a total of $1 \cdot 2 \cdot 4 \cdot 8 \cdot 6 = 384$ combinations. These are perfectly sound from a scientific perspective, but cannot be executed in current versions of TopSpin as the parameter NBL (number of modules) has a maximum value of 5.
4. NOAH-2 or NOAH-3 combinations consisting of the HMBC module directly followed by a $^1\text{H}-^1\text{H}$ homonuclear module: 18. These can be run, but are likely to produce lower-quality homonuclear spectra as the HMBC module dephases bulk magnetisation.
5. Duplicate, identical combinations where the same $^{13}\text{C}-^1\text{H}$ module (e.g. HSQC) was selected either from the third or the fourth column. There are 4 such modules, so we must subtract $2 \cdot 3 \cdot 4 \cdot 19 = 456$ combinations.
 - Note, however, that some of these duplicate combinations were *already* rejected in step (2) above. Thus, we need to add back 4 “NOAH-1” combinations that we double-counted.

This yields a total number of $5130 - 1 - 33 - 384 - 18 - 456 + 4 = 4242$ possible NOAH supersequences. Note that, unlike the original paper,¹ this does not take into account options that are set using acquisition flags, such as multiplicity editing in HSQC-type experiments and

inversion of “indirect” responses in HSQC-COSY and HSQC-TOCSY spectra. This also does not include modules that are only available via the “developer mode” interface.

S2 More HMBC artefact comparisons

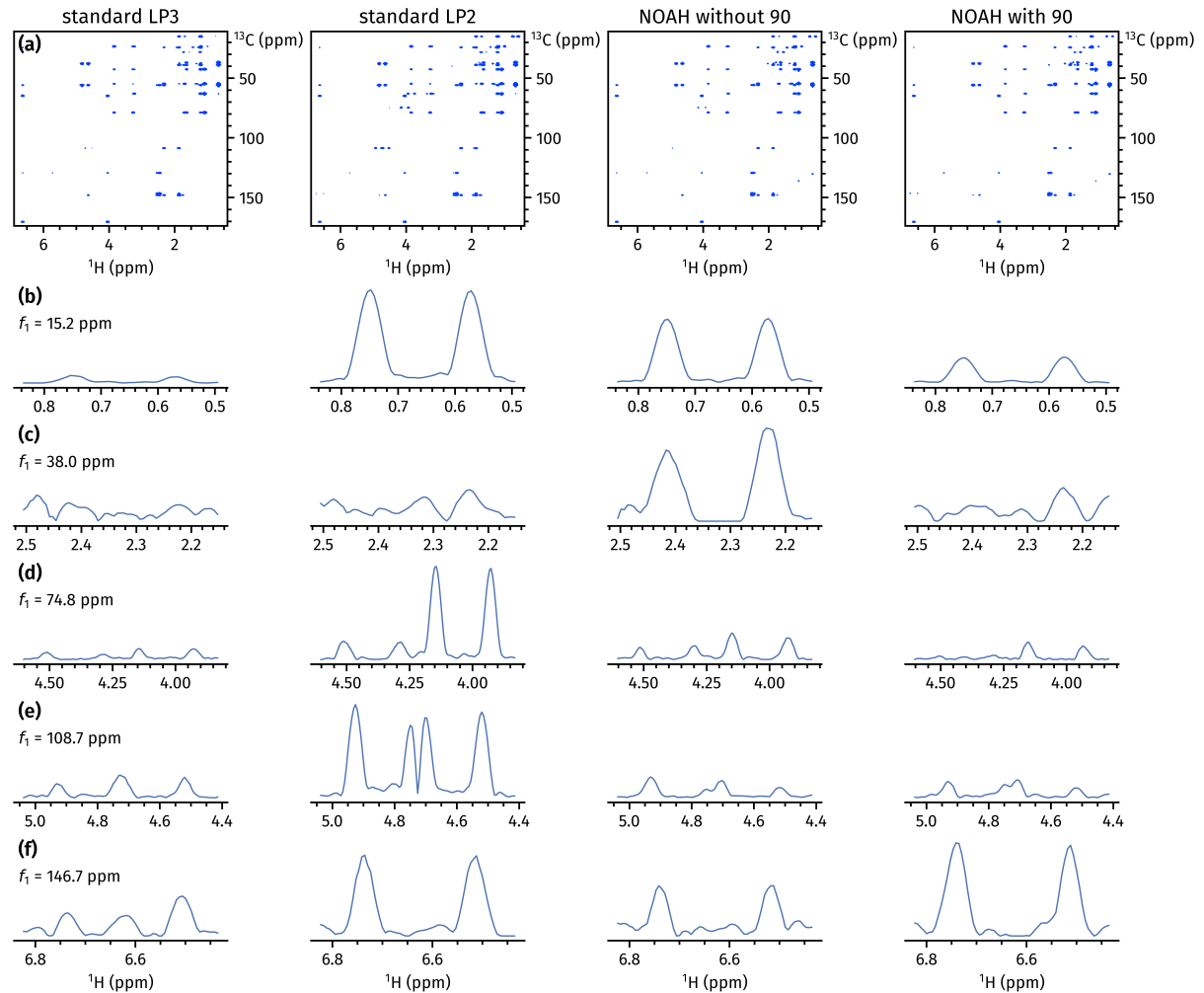


Figure S1: Comparisons of HMBC spectra obtained using the Bruker standard library sequences² `hmbcetgpl2nd` (with a third-order LPJF, first column); `hmbcetgpl2nd` (with a second-order LPJF, second column); and the NOAH *zz*-HMBC module (Figure 5a), before and after the added ${}^{13}\text{C}$ 90° pulse (third and fourth columns respectively). **(a)** The full 2D spectra, plotted with the same contour levels. **(b)–(f)** Multiple f_1 traces through the 2D spectra showing the ${}^1\text{J}_{\text{CH}}$ artefacts. Each row is plotted with the same y-axis range. In all cases except (f), the addition of the 90° pulse leads to far better artefact suppression; in many cases, its performance is comparable to the standard library third-order LPJF. Spectra were obtained on a 700 MHz Bruker AV III equipped with a TCI H/C/N cryoprobe; the sample used was 40 mM andrographolide in DMSO- d_6 .

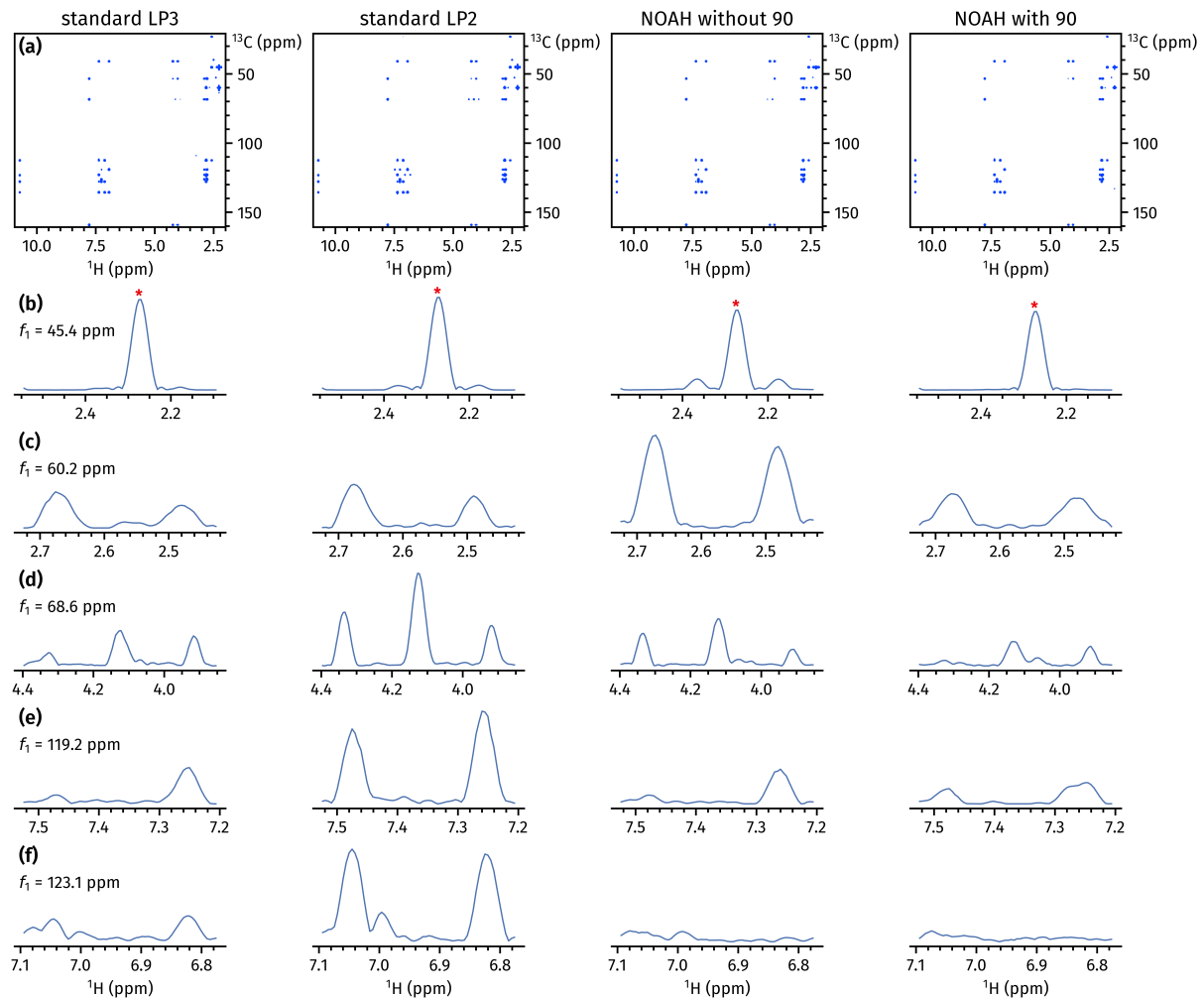


Figure S2: The same as in Figure S1, but instead acquired with a sample of 50 mM zolmitriptan in $\text{DMSO}-d_6$. Note that the peak labelled with an asterisk in (b) is a genuine correlation. It is, however, flanked by a pair of $^1J_{\text{CH}}$ artefacts (most visible in the third column, i.e. NOAH zz -HMBC without added 90° pulse).

S3 HMQC sensitivity comparison

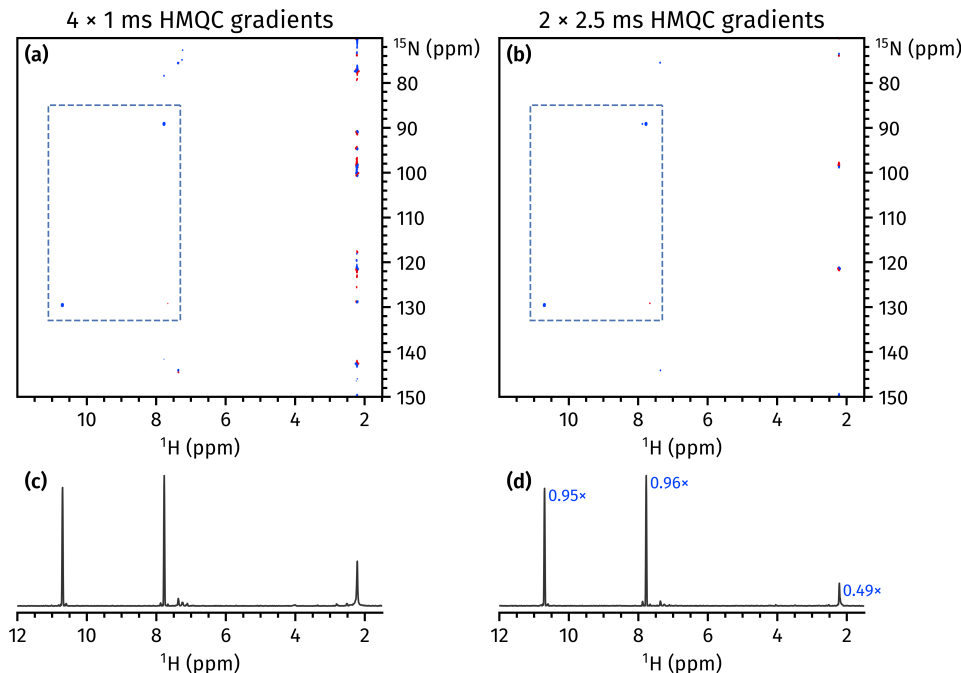


Figure S3: Comparisons of ^1H - ^{15}N HMQC spectra obtained using the two gradient schemes shown in Figure 6. (a)-(b) Full 2D spectra. The two desired signals are boxed. Note the artefacts at $f_2 = 2.2$ ppm; these arise from bulk magnetisation that is not fully dephased by the gradients in the HMQC module. (c)-(d) Positive projections of the spectra onto the f_2 axis. The relative intensities of the peaks and artefacts are shown in (d). Switching to the improved gradient scheme leads to no significant change in the intensity of the desired peaks ($\geq 95\%$), and halves the artefact intensity. We previously reported similar results with the ^1H - ^{15}N seHSQC module.³ Spectra were obtained on a 700 MHz Bruker AV III equipped with a TCI H/C/N cryoprobe; the sample used was 50 mM zolmitriptan in $\text{DMSO}-d_6$.

References

- (1) Kupče, Ě.; Claridge, T. D. W. *Angew. Chem. Int. Ed.* 2017, 56, 11779–11783, DOI: [10.1002/anie.201705506](https://doi.org/10.1002/anie.201705506).
- (2) Cicero, D. O.; Barbato, G.; Bazzo, R. *J. Magn. Reson.* 2001, 148, 209–213, DOI: [10.1006/jmre.2000.2234](https://doi.org/10.1006/jmre.2000.2234).
- (3) Yong, J. R. J.; Hansen, A. L.; Kupče, Ě.; Claridge, T. D. W. *J. Magn. Reson.* 2021, 329, 107027, DOI: [10.1016/j.jmr.2021.107027](https://doi.org/10.1016/j.jmr.2021.107027).